Excitation power dependent population pathways and absolute quantum yields of upconversion nanoparticles in different solvents

-Supporting Information-

*Christian Würth[1,a], Martin Kaiser[1,a], Stefan Wilhelm[2], Bettina Grauel, Thomas Hirsch[2], Ute Resch-Genger**

Analytical characterization of the UCNP.

A single large batch of high quality 23 nm-sized oleate (OA)-coated $NaYF_4(Yb^{3+}/Er^{3+})$ UCNPs was prepared with a narrow size distribution (average diameter 22.7 ± 0.7 nm; see Figure S1), uniform shape, and pure hexagonal (β-phase) crystal structure (Figure S2), and a solvodynamic diameter of 29 ± 3 nm in cyclohexane (dynamic light scattering (DLS); intensity-weighted size distribution; see Figure S3) as recently described.[1] The lanthanide ions content of the UCNPs was determined by inductively coupled plasma optical emission spectrometry (ICP-OES) to 78.4 ± 0.1 mol-% for Y^{3+}, 19.3 ± 0.1 mol-% for Yb^{3+}, and 2.3 ± 0.1 mol-% for Er^{3+}, respectively. Thermal gravimetric analysis (TGA) of the OA-capped UCNPs yielded a mass loss of 9.1% equaling a ligand density of $5.7x10^3$ OA ligands per UCNP (equalling 3.5 OA ligands per nm^2 of the UCNP surface area) and a ligand coating of the UCNP surface of about 70%. Subsequent surface modifications for UCNPs in polar environments like polar and aprotic DMF, water, and D_2O included exchange of OA for BF_4^- and citrate and encapsulation by exemplary chosen amphiphilic DSPE (1,2-distearoyl-sn-glycero-3-phospho-ethanolamine-N-[methoxy(polythylene glycol)-2000] (ammonium salt)). The colloidal stability of all UCNP dispersions was confirmed by DLS measurements (see Figure S3) yielding hydrodynamic diameters of the differently functionalized UCNP of 24 nm (ligand BF_4^-, solvent DMF), 24 nm (ligand citrate, solvent water, pH 7, Zeta potential -25 mV; electrostatic stabilization), and 53 nm (ligand DSPE, solvent water, pH 7, Zeta potential -9 mV; mainly steric stabilization), respectively.

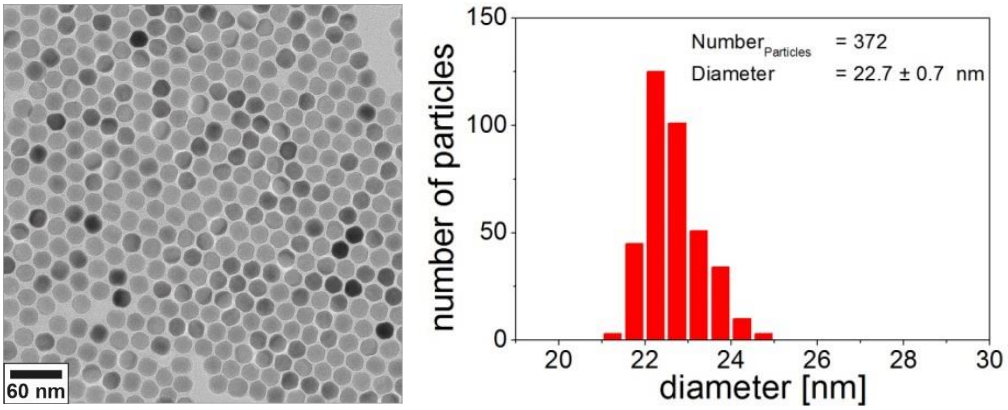

Figure S1. Left: TEM image of OA-coated β-$NaYF_4(Yb^{3+},Er^{3+})$ UCNPs. Right: Size distribution histogram. TEM image analysis of 372 particles using ImageJ software revealed a particle diameter of 22.7 ± 0.7 nm.

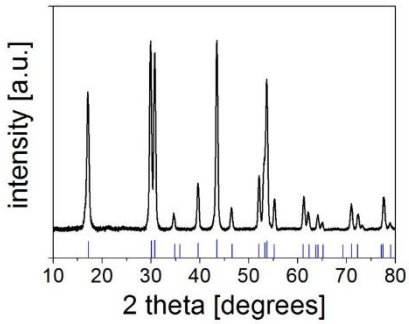

Figure S2. X-ray powder diffraction (XRD) diagram of β-$NaYF_4$(Yb^{3+},Er^{3+}) UCNPs. The blue lines indicate the diffraction peaks of hexagonal (β-phase) $NaYF_4$ (XRD standard pattern; ICDD PDF #16-0334).

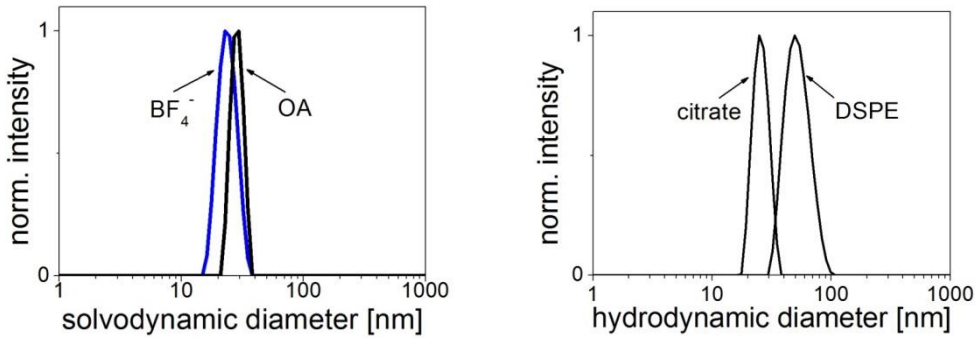

Figure S3. Left: Solvodynamic diameters of OA-coated UCNPs dispersed in cyclohexane (29 ± 3 nm) and BF_4^- stabilized UCNPs in DMF (24 ± 4 nm), respectively. Right: Hydrodynamic diameters of citrate-coated UCNPs (24 ± 3 nm) and DSPE-coated UCNPs (53 ± 5 nm) in water, respectively.

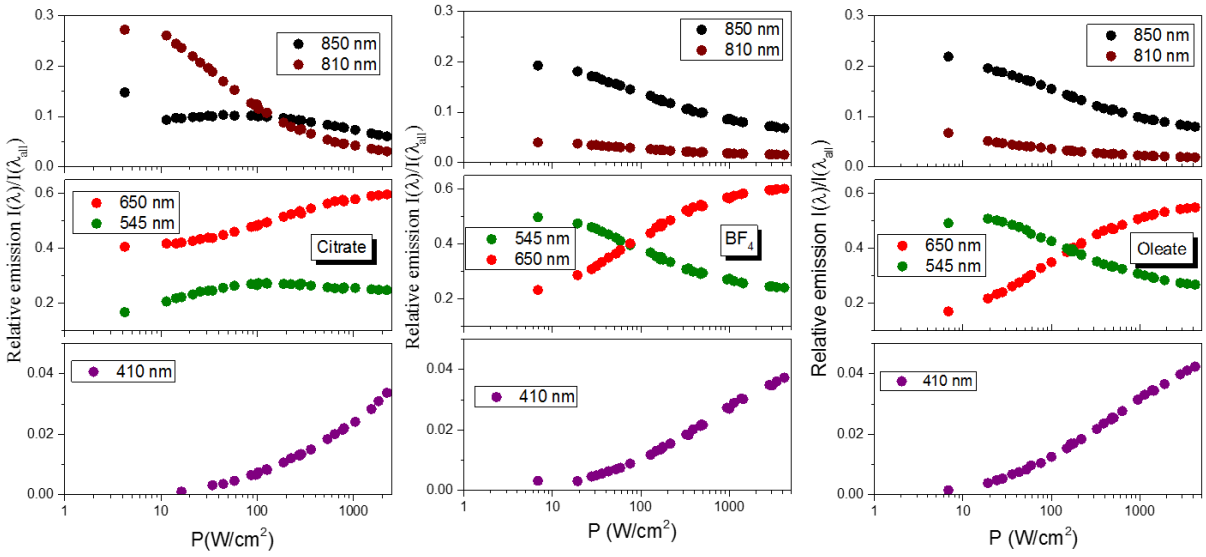

Figure S4. Contribution of the integral photon fluxes of the different UC emission bands $I(\lambda)$ to the overall integral intensity $I(\lambda_{all})$ of the UC emission for citrate-stabilized UCNP in water (left panels), BF_4^--stabilized UCNP in DMF (middle panels), and OA-capped UCNP in cyclohexane (right panels), respectively. Crossing points indicate matching photon fluxes.

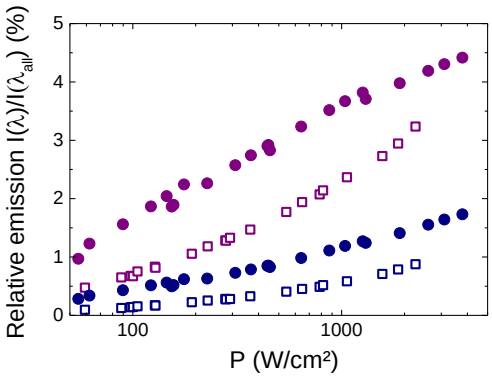

Figure S5. Contribution of the integral photon fluxes of the of the 410 nm and 360 nm emission bands $I(\lambda)$ to the overall integral UC photon flux $I(\lambda_{all})$ of the UC emission for DSPEstabilized UCNP in water (open symbols) and D_2O (solid symbols).

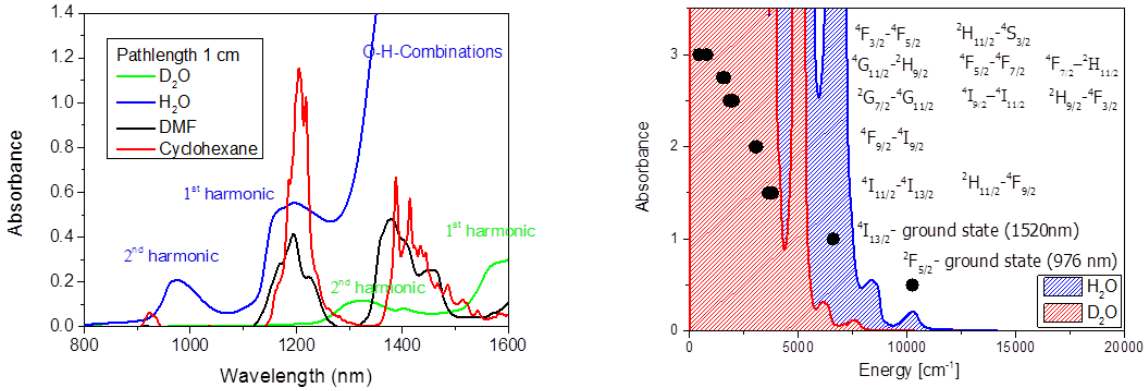

Figure S6. Left panel: Absorption spectra of the different solvents used for UCNP dispersion. Right panel: Comparison of the energies of water vibrations and Er^{3+} transitions.

Consideration of solvent absorption and heating effects on Φ_{UC} in water.

In contrast to cyclohexane, DMF, and D_2O, water can absorb radiation with a wavelength of 980 nm (see Figure S6). In water, i.a., within an optical pathlength of 1 cm as used by us for our luminescence measurements, about 40% of the incident photon flux is absorbed by the solvent,[2] with the absorbed energy being converted into heat. In order to account for a *P* reduction due to water absorption, *P* was rescaled for all measurements in water Moreover, the nonradiatively deactivated electronic states of the dispersed UCNP can give rise to a temperature increase of the samples during the measurement/illumination time. In order to determine the temperature of the UCNP dispersions, we assumed the same *P*-dependence of the $^4S_{3/2}$ and $^2H_{11/2}$ levels and used a calibration of the temperature dependent green-green ration of the DSPE stabilized UCNP in water and D_2O. With this procedure, we obtained temperatures of ca. 35°C and ca. 65°C for D_2O and water for the highest *P* used here. Subsequently, temperature dependent measurements of the integral upconversion luminescence were performed witha fluorometer in 0/90° measurement geometry with low *P* excitation to determine relatively the size of the temperature induced diminution in Φ_{UC}. Based upon these measurements, the decrease in Φ_{UC} was estimated to 10% for nonabsorbing organic solvents and D_2O and 25% for absorbing water at the highest *P* used.

As follows from the Φ_{UC} measurements, the slope of $\Phi_{UC}(P)$ of our UCNPs in water and in organic solvents is nearly independent of *P*. Therefore, the temperature-induced changes in population rates and $\Phi_{UC}(P)$ are small compared to the population rates induced by photon absorption/photoexcitation.

In addition, time-resolved measurements of the Yb^{3+} luminescence at 980 nm shown in Figure S8 reveal that the luminescence lifetime of Yb^{3+} is not affected by temperature, indicating that temperature-induced nonradiative relaxation is mainly favored for Er^{3+} energy levels.

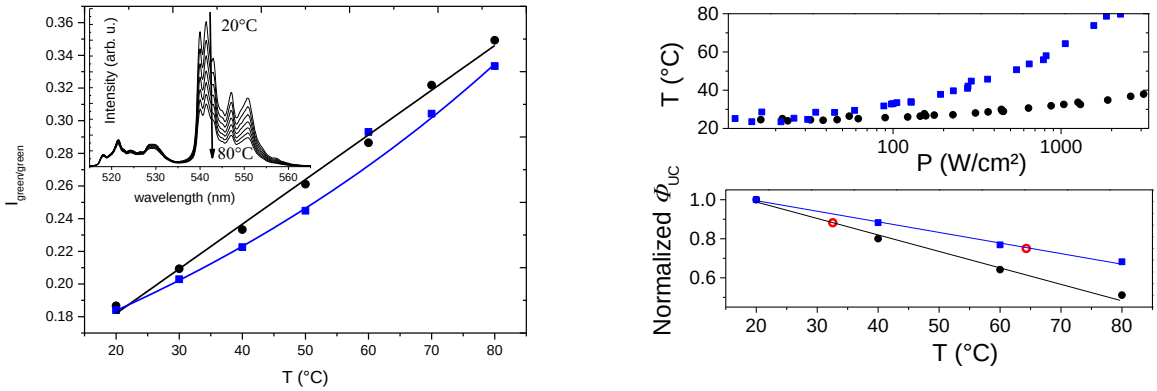

Figure S7. Left: Temperature dependent green-green ($I_{green/green}$ = *I*(525nm)/*I*(545nm)) ratio for DSPE-stabilized UCNP in water (blue) and D_20 (black). Right, top: Estimation of the *P*-dependent temperature increase. Right, bottom: Estimation of the temperature-dependent decrease of Φ_{UC}.

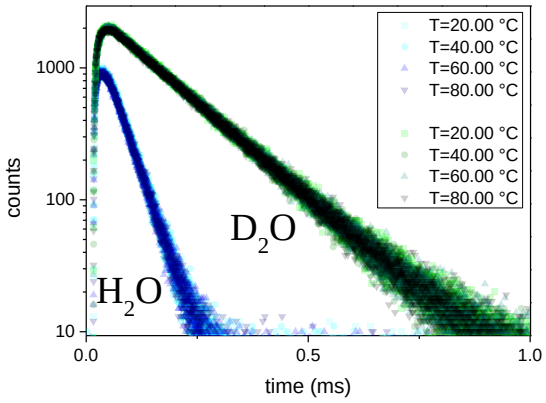

Figure S8. Luminescence decay kinetics of DSPE-stabilized UCNPs in water and D_2O at different temperatures; λ_{ex} = 940 nm, λ_{em} = 980 nm (Yb^{3+} luminescence).

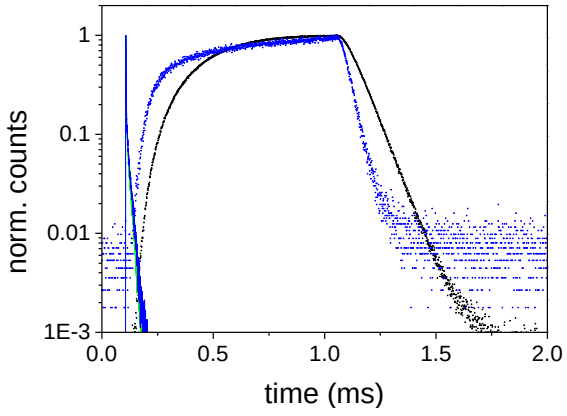

Figure S9. Luminescence decay kinetics of up- (symbols) and downconversion (lines) processes in DSPE-stabilized UCNP dispersed in water (blue) and D_2O (black) for λ_{em} = 410 nm; excitation of the UC and DC luminescence was at 976 nm and 365 nm, respectively.

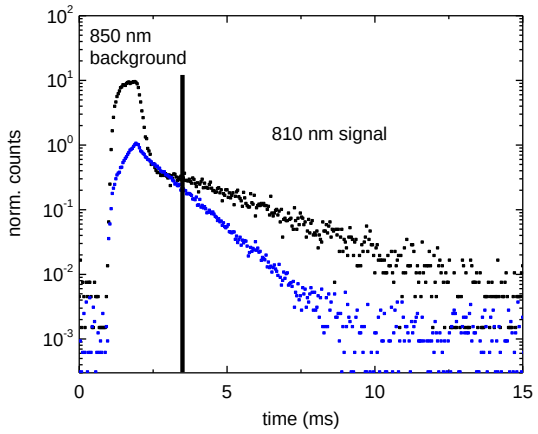

Figure S10. Luminescence decay kinetics of DSPE-stabilized UCNP dispersed in water (blue) and D_2O (black) for λ_{em} = 810 nm; excitation was at 976 nm. In D_2O, the 810 nm emission is very weak and strongly overlaps with the 850 nm emission band.

Determination of lifetime components

Fitting of the luminescence kinetics of UCNP is challenging due to the complex rise and decay behavior. Usually, a tail fit is done for accessing lifetimes. Critical can be here that shortly after the laser pulse, still a significant energy transfer occurs within a short time interval due to the long lifetimes of the lanthanide emitters. This was considered by omitting the first data points of the measured decay curves. This implies, however, that the amplitudes determined with this fitting procedure deviate from the true values. In order to account for such effects, for multi-exponential decay kinetics, we distinguish solely between high (> 65 %) and very high (> 90 %) amplitudes. In order to obtain reliable fit results, two special cases have to been considered: a) In the case of a very low amplitude long lifetime component, the small signal to noise leads to fits strongly underestimating long lifetimes values for the tail fit. This can be circumvented by dividing the fitting range in two parts for short and long lifetime components and perform the tail fit separately for each lifetime component. b) The determination of the short lifetime component of the DC decay curves requires only fitting of the onset of the decay. Due to its strongly multi-exponential behavior, fitting of the complete decay curve is not recommended. In order to control the quality of the obtained lifetime data, we also determined the derivation of the decay curve $\tau_m(t)$, see equation 1.

$$\tau_{M(t=\frac{t_2-t_1}{2})}=\frac{t_2-t_1}{\ln(I_2)-\ln(I_1)}\,, \qquad \text{(eq. 1)}$$

Here I_1, I_2 and t_1, t_2 are the neighboring intensity and time values, respectively. The short lifetime component τ_1 equals the first minima $\tau_M(t)$, and is in excellent agreement with the fit results (deviation < 5 %). The long lifetime component τ_2 can be found where the $\tau_M(t)$ is constant. This value is also in good agreement with the fit results (deviation < 20 %).

Table S1: Fit results of luminescence decays of DSPE stabilized UCNP in water and D_2O.

		Upconversion				Downconversion				
Solvent	Lifetime	410 nm	545 nm	655 nm	810 nm	410 nm	545 nm	655 nm	930 nm	1520 nm
H_2O	τ_1 (µs)	40	69 (high)	185 (high)	1100	16	45 (high)	140 (high)	42 (very high)	2100 (very high)
	τ_2 (µs)		740	730			n.d.	n.d.	1200	3400
D_2O	τ_1 (µs)	74	120 (very high)	180 (very high)	2800	15	65 (high)	110 (high)	160 (very high)	1400
	τ_2 (µs)		3000	3100	-		n.d	n.d.	2900	4400 (very high)

n.d. :could not be determined, since the deriviation of the decay curve shows no convergence

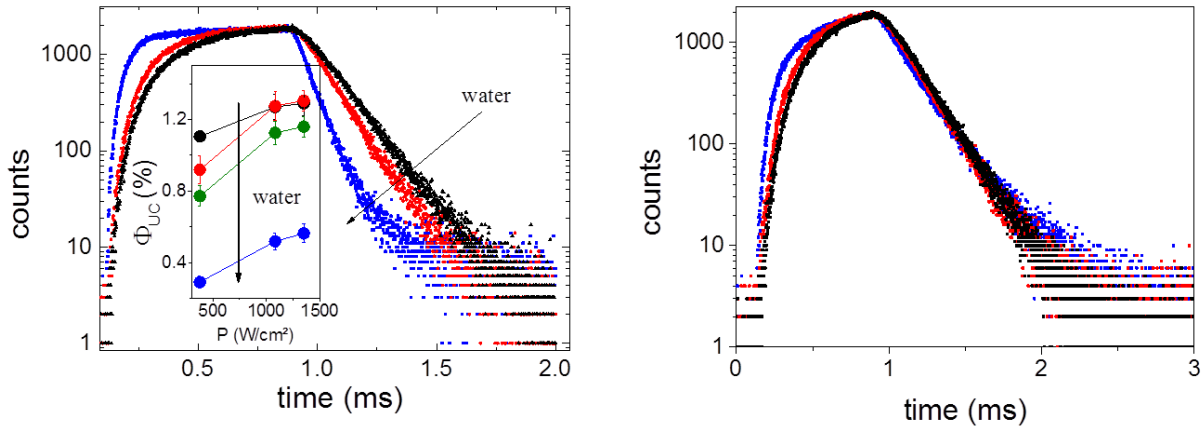

Figure S11. Luminescence rise and decay behavior of OA-capped UCNP in cyclohexane and citrate-stabilized UCNP in mixtures and pure water and D_2O (100 % H_2O: blue; 5 % H_2O, 95 % D_2O: red; < 1 % H_20, > 99 % D_2O: black) for λ_{em} = 545 nm (left) and 655nm (right). The inset shows the $\Phi_{UC}(P)$ for citrate-stabilized UCNP in mixtures of water and D_2O (< 1% H_20, > 99% D_2O: black), (5% H_20, 95% D_2O: red), (10% H_20, 90% D_2O: green), (100% H_2O: blue).

Table S2: Fit results of luminescence decays of Citrate-capped UCNP in different D_2O/H_2O mixtures

Citrate-capped UCNP in D_2O/H_2O	Lifetime	545 nm	655 nm
0/100	τ_1 (µs)	60 (very high)	180 (very high)
	τ_2 (µs)	n.d	n.d.
95/5	τ_1 (µs)	110	180
> 99/< 1%	τ_1 (µs)	130	180

n.d. :could not be determined, since the derivation of the decay curve shows no convergence

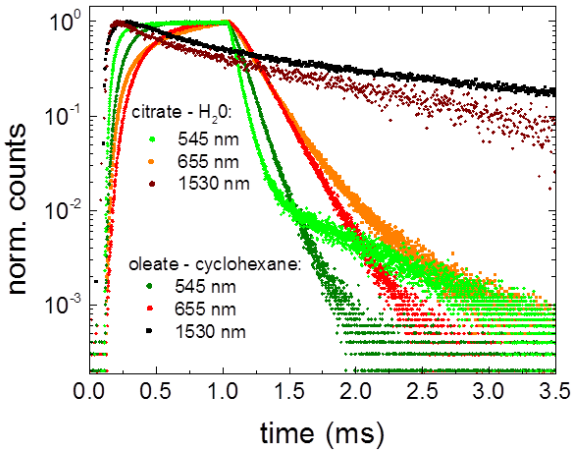

Figure S12. Rise and decay behavior of OA-capped UCNP in cyclohexane and citrate-stabilized UCNP in pure water measured at different emission bands: λ_{em} = 545 nm, λ_{em} = 655 and λ_{em} = 1520 nm, respectively. Excitation was at 980 nm.

Table S3: Fit results of luminescence decays of differently stabilized UCNP in different solvents.

Stabilizing ligand	Lifetime	545 nm	655 nm	1520 nm
Citrate Solvent: H_2O	τ_1 (µs)	62	180 (high)	750
	τ_2 (µs)	630	600	1750 (high)
Oleate Solvent: cyclohexane	τ_1 (µs)	97 (high)	170	180
	τ_1 (µs)	n.d.		770
BF_4^- Solvent: DMF	τ_1 (µs)	95	240	180
	τ_2 (µs)			750

n.d. :could not be determined, since the derivation of the decay curve shows no convergence.

Model of the Population Dynamics in Yb^{3+}-Er^{3+} co-doped UCNPs

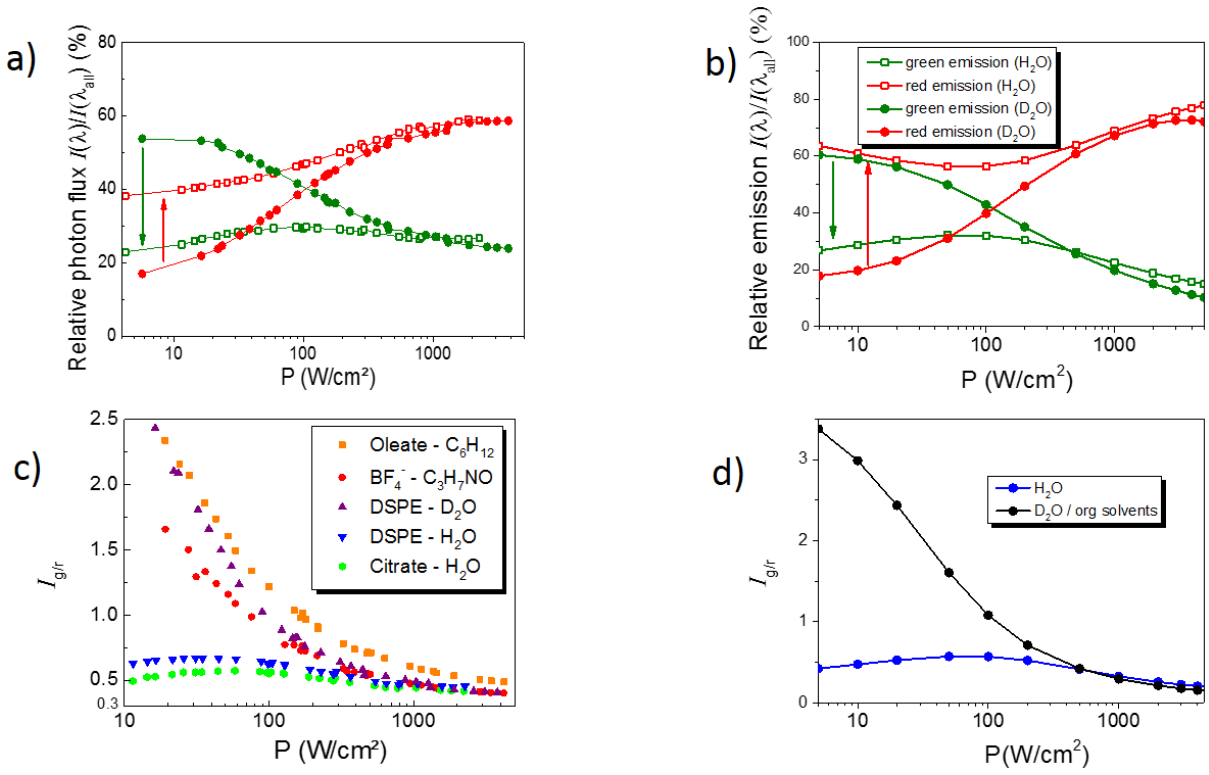

Figure S13: a) Measured relative emission intensities of the red and green emission for UCNPs in water (open symbols) and organic solvents (solid symbols). b) Calculated relative emission intensities of the red and green emission for UCNPs in water (open symbols) and organic solvents (solid symbols). c) Measured *P*-dependence of $I_{g/r}$ for OA-capped UCNPs in cyclohexane, citrate-stabilized UCNPs in water, and DPSE-stabilized UCNPs in water and D_2O, respectively. d) Calculated green-red ratio ($I_{g/r}$) for UCNPs in water (blue) and organic solvents (black).

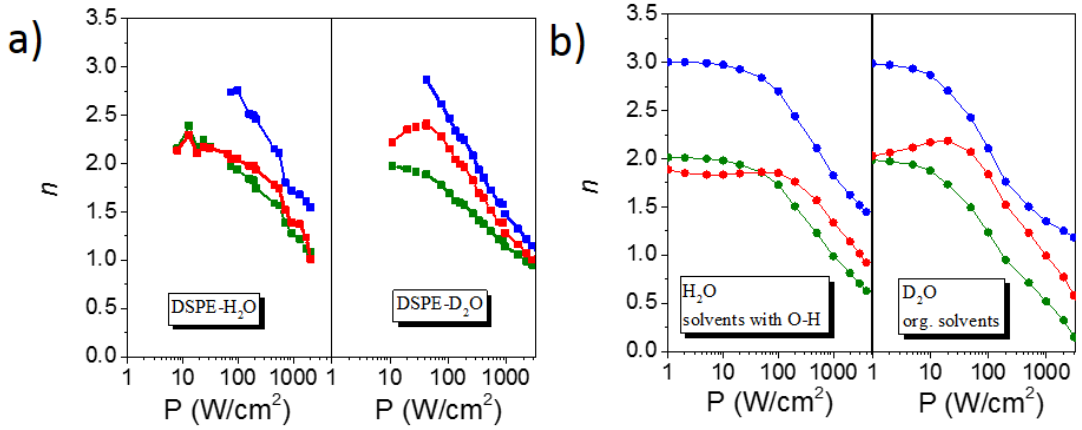

Figure S14: a) Measured slope factors for UCNPs in organic solvents and water right for the blue, red and green emission bands. b) Calculated slope factors for UCNPs in organic solvents and water right for the blue, red and green emission bands.

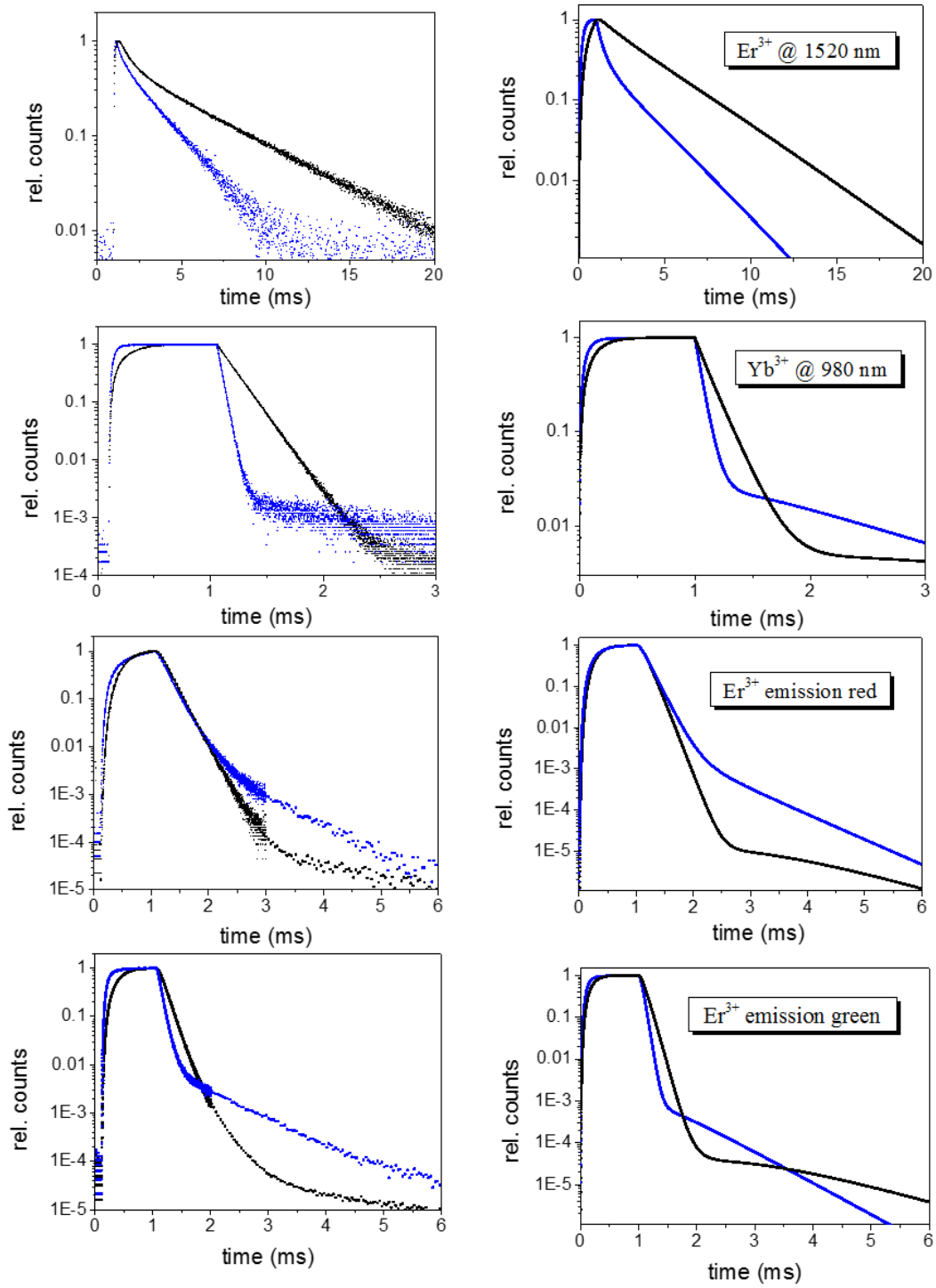

Figure S15: Calculated decay curves of UCNPs in water (blue) and organic solvents (black).

(1) Wilhelm, S.; Kaiser, M.; Würth, C.; Heiland, J.; Carrillo-Carrion, C.; Muhr, V.; Wolfbeis, O. S.; Parak, W. J.; Resch-Genger, U.; Hirsch, T. *Nanoscale* **2015**, *7*, 1403.

(2) Hatami, S.; Wurth, C.; Kaiser, M.; Leubner, S.; Gabriel, S.; Bahrig, L.; Lesnyak, V.; Pauli, J.; Gaponik, N.; Eychmuller, A.; Resch-Genger, U. *Nanoscale* **2015**, *7*, 133.

(3) Anderson, R. B.; Smith, S. J.; May, P. S.; Berry, M. T. *Journal of Physical Chemistry Letters* **2014**, *5*, 36.